Simulation and theory of a model for tetrahedral colloidal particles

G. Munaó,[1,2,a)] D. Costa,[1] F. Sciortino,[2] and C. Caccamo[1]
[1]*Dipartimento di Fisica and CNISM, Università degli Studi di Messina Viale F. Stagno d'Alcontres 31, 98166 Messina, Italy*
[2]*Dipartimento di Fisica and CNR-ISC, Università di Roma "La Sapienza" Piazzale Aldo Moro 2, 00185 Roma, Italy*

(Received 15 March 2011; accepted 6 April 2011; published online 17 May 2011)

We study the thermodynamic and structural properties of a five-site tetrahedral molecular model by means of different Monte Carlo simulation techniques, and the reference interaction site model (RISM) theory of molecular fluids. Simulations and theory signal the onset, at sufficiently low temperatures, of two different tetrahedral molecular arrangements, with a more open topology progressively giving place to a fully bonded one, as the temperature decreases. The RISM theory reproduces the splitting of the static structure factor at low temperatures, a feature intimately related to the onset of the tetrahedral ordering. Less accurate predictions are obtained for the liquid-vapor coexistence and the short-range correlations. © *2011 American Institute of Physics*. [doi:10.1063/1.3582904]

I. INTRODUCTION

Advanced synthesis protocols offer nowadays the opportunity to produce colloidal molecules with well-defined shape and tunable patchiness.[1–4] This new generation of colloids is expected to provide the building blocks of self-assembling materials, and to give rise to a rich and still unexplored variety of supra-colloidal structures.

In parallel with the experimental development, significant theoretical and numerical efforts are currently promoted to predict the structural and collective properties of colloidal particles[5–7] characterized by shape anisotropies or asymmetrically patterned interactions.[8–10] In order to develop accurate theoretical methods, effective potentials and more elementary, "primitive" models, [11–14] often resembling the corresponding molecular ones[15,16] (see Ref. 17 for a recent review), are under scrutiny. Integral equation theories[18] may play in this context a significant role, being relatively simple to implement and generally providing accurate results when applied to the description of fluid phase equilibria.[19] As an example, the reference hypernetted chain scheme[20] and a thermodynamic perturbation theory,[21,22] were used to investigate one- and two-patch fluid models.[6,14] In the case of the more asymmetric one-patch model, the theoretical approach does not succeed in reproducing the system structure, when self-assembly into micelles and vesicles takes place.[7] Similar difficulties were also experienced in early attempts to reproduce the tetrahedral order observed in associating liquid models,[23] with the split of the main peak of the static structure factor upon cooling hardly reproduced. An appropriate tool to describe distributed-site, patchy or patterned interactions is constituted by the reference interaction site model (RISM) theory, developed in the early 1970s by Chandler and Andersen[24] as a generalization of the Ornstein-Zernike theory of simple fluids[18] able to describe the structure of molecular liquids. In the initial formulation, molecules were viewed as composed by a suitable superposition of several hard spheres, rigidly bonded together to represent a given molecular geometry.[25] Later on, the theory was extended to deal with more realistic representation of complex liquids, including associating fluids such as water,[26,27] methanol,[28–30] and their mixtures.[31] In the context of colloids, RISM was used, e.g., to study the thermodynamic and structural properties of discotic lamellar colloids,[32,33] the self-assembly in diblock copolymers (modeled as "ultrasoft" colloids),[34] the interaction between colloidal particles and macromolecules[35] and the crystallization and solvation properties of nanoparticles in aqueous solutions[36] (see also the reviews in Refs. 37 and 38 and Refs. 39 and 40 for recent advances).

In this work we assess the ability of the RISM to predict the properties of colloidal systems in which the microscopic interaction combines together bonding effects and the tendency to form a local tetrahedral network. Our theoretical predictions are complemented by Monte Carlo (for the structure), Gibbs Ensemble (for the liquid-vapor coexistence) and grand canonical Monte Carlo (for the liquid-vapor critical point) simulations. Simulations, besides providing a microscopic insight of the system, constitute the necessary benchmark to assess the accuracy of the theory.

The model we propose envisions five interaction sites, rigidly arranged at the center and the four vertices of a regular tetrahedron. All sites on different molecules interact through a hard core potential; an additional square-well attractive interaction is introduced between the center of one molecule and any of the four equivalent external sites of another molecule. The proposed geometry, where four external spheres are partially fused with a central one (see Fig. 1), closely resembles a colloidal molecule recently synthesized by means of a novel technique, in which cross-linked particles with a liquid protrusion, assemble by coalescence of the protrusion itself.[1] The geometry of the model, combined with the proposed site-site potentials, favor a high directionality of interactions and the formation of a limited number of possible bonds. Such "limited-valence" class of models has received a significant attention in the last years; in particular, on decreasing the valence below six, it has been demonstrated that the

a)Electronic mail: gmunao@gmail.com.

liquid-vapor unstable region progressively shrinks to lower densities, creating an intermediate region where a stable network may be formed,[41,42] giving rise to equilibrium gels.[43] Finally, our model, in which the protrusions repel each other and are attracted only by the exposed surface of the central particle, provides also an example of the recently investigated "inverse patchy colloids."[44]

The paper is organized as follows: in Sec. II we describe the model, the RISM theory, and the plan of simulations. Results are presented and discussed in Sec. III. Conclusions follow in Sec. IV.

II. MODEL, THEORY, AND SIMULATION APPROACHES

In the tetrahedral model depicted in Fig. 1 we label with 1 the central sphere (with its diameter σ_1 constituting the length scale of the model) and with 2 any of the four equivalent external spheres (with diameter $\sigma_2 = 0.80\sigma_1$). The distance between the center of the molecule and one of the vertices is $L_{12} = 0.55\sigma_1$. In our model, the external spheres partially overlap with the central one but do not intersect each other. Hence, the molecular volume V_M is given by the total volume of the five spheres, minus four times the intersecting region (constituted by the union of two different spherical caps) of one external sphere with the central one; we obtain for the proposed geometry $V_M = 1.3015\,\sigma_1^3$, and we shall use, as a dimensionless measure of the density of the system, the packing fraction $\eta = \rho V_M$, where ρ is the (molecular) number density of the system. Sites 1 on different molecules interact via a purely hard-sphere interaction (with diameter σ_1), and the same holds for the interaction among spheres 2 (with diameter σ_2); the cross interaction 1-2 contains also a square-well attraction, immediately next to the hard-sphere repulsion, assuming the form:

$$U_{12}(r) = \begin{cases} \infty & \text{if } r < \sigma_{12} \equiv (\sigma_1 + \sigma_2)/2 \\ -U_0 & \text{if } \sigma_{12} < r < \lambda + \sigma_{12} \\ 0 & \text{if } r > \lambda + \sigma_{12} \end{cases}, \qquad (1)$$

where r is the distance between sites 1 and 2 and the (narrow) attractive range is fixed at $\lambda = 0.027\sigma_1$. The interaction potential between two generic molecules i and j has a minimum $-2U_0$, in the configurations where the central sphere of i is bonded to an external sphere of j and vice versa. The model potential parameters have been selected with the aim of favoring a limited-valence coordination[23] via double bonds. The potential depth U_0 constitutes the natural energy scale of the system, with the reduced temperature defined as $T^* = k_B T/U_0$.

In the RISM framework, the pair structure of a fluid composed by identical molecules, each formed by n interaction sites ($n = 5$ in our case), is characterized by a set of $n(n+1)/2$ site-site intermolecular pair correlation functions $h_{\alpha\eta}(r) = g_{\alpha\eta}(r) - 1$, where $g_{\alpha\eta}(r)$ are the site-site radial distribution functions. The $h_{\alpha\eta}(r)$ are related to a set of intermolecular direct correlation functions $c_{\alpha\eta}(r)$ by a matrix equation that in k-space reads

$$\mathbf{H}(k) = \mathbf{W}(k)\mathbf{C}(k)\mathbf{W}(k) + \rho\mathbf{W}(k)\mathbf{C}(k)\mathbf{H}(k)\,. \qquad (2)$$

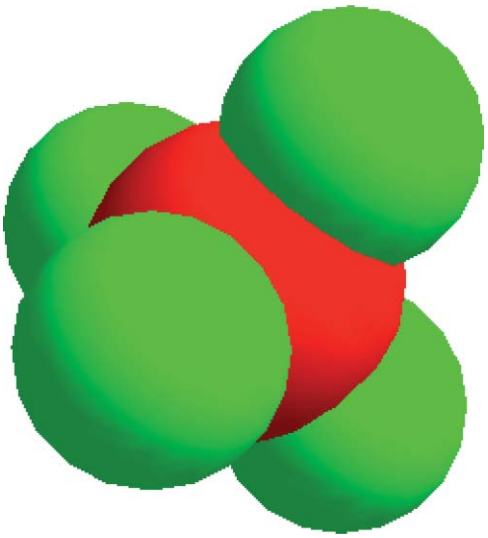

FIG. 1. Geometry of the molecular model studied in this work; different colors are used for the central core and the four equivalent protrusions.

In Eq. (2), $\mathbf{H} \equiv [h_{\alpha\eta}(k)]$, $\mathbf{C} \equiv [c_{\alpha\eta}(k)]$, and $\mathbf{W} \equiv [w_{\alpha\eta}(k)]$ are $n \times n$ symmetric matrices; the elements $w_{\alpha\eta}(k)$ are the Fourier transforms of the intramolecular correlation functions; provided the particles are rigid, we have explicitly

$$w_{\alpha\eta}(k) = \frac{\sin[kL_{\alpha\eta}]}{kL_{\alpha\eta}}\,, \qquad (3)$$

where $L_{\alpha\eta}$ is the distance between a pair of sites α and η belonging to the same molecule. The RISM equation has been complemented by the hypernetted chain (HNC) closure[45] for the direct correlation functions $c_{\alpha\eta}(r)$:

$$c_{\alpha\eta}(r) = \exp[-\beta U_{\alpha\eta}(r) + \gamma_{\alpha\eta}(r)] - \gamma_{\alpha\eta}(r) - 1, \qquad (4)$$

where $U_{\alpha\eta}(r)$ is the intermolecular pair potential and the gamma functions are defined as: $\gamma_{\alpha\eta}(r) = h_{\alpha\eta}(r) - c_{\alpha\eta}(r)$. We have also tested the Percus-Yevick (PY) closure

$$c_{\alpha\eta}(r) = \{1 - \exp[\beta U_{\alpha\eta}(r)]\} g_{\alpha\eta}(r). \qquad (5)$$

As it is known, the PY yields an overall good description of liquid structure and thermodynamics of the atomic square-well fluids.[46,47]

The perfect equivalence of the four external interaction sites allows one to derive a contracted version of the RISM formalism,[48] where only one of such identical sites is explicitly considered, and hence the dimension of all correlation matrices reduces from 5×5 to 2×2. In particular, the "symmetry-reduced" intramolecular correlations $\overline{\mathbf{W}}(k)$ read as

$$\overline{\mathbf{W}}(k) \equiv [\overline{w}_{IJ}(k)] = \frac{1}{n_I}\sum_{i\in I}[w_{ij}(k)],$$

$$= \frac{1}{n_J}\sum_{j\in J}[w_{ij}(k)] = [\overline{w}_{JI}(k)], \qquad (6)$$

where the indices I and J refer to the non-equivalent types of interaction sites (i.e., 1 and 2 in this work), and n_I and n_J are their corresponding multiplicity (one and four for sites of type

1 and 2, respectively). The reduced matrix $\overline{\mathbf{C}}(k)$ has elements: $[\overline{c}_{IJ}(k)] = n_I[c_{IJ}(k)]n_J$.[48]

As for the calculation of the free energy and pressure within the RISM/HNC formalism (to be used for the determination of the liquid-vapor phase coexistence), closed local formulæ (i.e., not requiring a thermodynamic integration) were derived by Singer and Chandler,[49] closely following the corresponding relations deduced for the HNC theory of simple fluids:[50]

$$-\frac{\beta A^{\mathrm{ex}}}{N} = \frac{\rho^2}{2}\sum_{\alpha,\beta}\int \mathrm{d}\mathbf{r}\left[c_{\alpha\beta}(r) - \frac{1}{2}h^2_{\alpha\beta}(r)\right] - \frac{1}{2(2\pi)^3}\int \mathrm{d}\mathbf{k}\,\{\mathrm{Tr}\rho\mathbf{W}(k)\mathbf{C}(k) + \ln\det[1-\rho\mathbf{W}(k)\mathbf{C}(k)]\}, \quad (7)$$

$$\frac{\beta P}{\rho} = 1 - \frac{\rho}{2}\sum_{\alpha,\beta}\int \mathrm{d}\mathbf{r}\left[c_{\alpha\beta}(r) - \frac{1}{2}h^2_{\alpha\beta}(r)\right] + \frac{1}{2(2\pi)^3}\int \mathrm{d}\mathbf{k}\{\rho^{-1}\ln\det[\mathbf{I}-\rho\mathbf{W}(k)\mathbf{C}(k)] + \mathrm{Tr}\,[\mathbf{W}(k)\mathbf{C}(k)][\mathbf{I}-\rho\mathbf{W}(k)\mathbf{C}(k)]^{-1}\}. \quad (8)$$

Occasionally, in order to improve the convergence of the RISM equation in the low-density regime, we have also adopted the partially linearized version of HNC, due to Kovalenko and Hirata,[51] which employs a combination of the mean spherical approximation (MSA) and of the HNC:

$$c_{\alpha\eta}(r) = \begin{cases} \text{HNC} & \text{if} \quad g_{\alpha\eta}(r) \le 1 \\ \text{MSA} & \text{if} \quad g_{\alpha\eta}(r) > 1. \end{cases} \quad (9)$$

We recall that within MSA

$$\begin{cases} g_{\alpha\eta}(r) = 0 & \text{if} \quad r \le \sigma_{\alpha\eta} \\ c_{\alpha\eta}(r) = -\beta U_{\alpha\eta} & \text{if} \quad r > \sigma_{\alpha\eta}. \end{cases} \quad (10)$$

The numerical solution of the RISM has been implemented through a standard iterative Picard algorithm, on a mesh of 2^{12} points with a spacing $\Delta r = 0.005\sigma_1$.[37]

Monte Carlo (MC) simulations at constant volume and temperature have been carried out on a sample composed of $N = 500$ molecules enclosed in a cubic box with standard periodic boundary conditions. We have covered a wide range of temperatures ($0.13 < T^* < 2$) and packing fractions ($0.013 < \eta < 0.442$). We have also performed Gibbs Ensemble Monte Carlo (GEMC) simulations to map the coexistence curve. The GEMC method was designed[52] to study coexistence in the region where the liquid-vapor free-energy barrier is sufficiently high to prevent crossing between the two phases. Using GEMC, we have studied a system of (total) 350 particles which partition themselves into the two boxes. At temperatures much less than the critical temperature, the vapor phase box contains only a few particles, while the remaining particles compose the liquid phase. To locate the position of the critical point, we have performed grand canonical Monte Carlo (GCMC) simulations[53] for a system of several sizes, up to box length of $10\sigma_1$. These calculations are complemented with histogram reweighting techniques to match the distribution of the order parameter $\rho - se$ with the known functional dependence expected for the Ising universality class critical point.[54] Here ρ is the number density, e is the potential energy density, and s is the mixing field parameter. In all simulations, translational and rotational moves consisted in a random translation between $\pm 0.05\sigma_1$ and a random rotation of ± 0.1 rad of a randomly selected particle. Depending on the MC method, insertion and deletion moves (or swap moves) have been attempted, on average every 400 displacement moves, and volume change moves (with volume changes of the order of $0.5\sigma_1^3$) every 2000 motion moves.

III. RESULTS AND DISCUSSION

In order to define the relevant temperature and density scales of the model, we have first evaluated the GEMC and RISM liquid-vapor coexistence curves and the corresponding critical points; results are reported in Fig. 2. The GCMC critical parameters have been estimated as: $T^*_{\mathrm{cr}} \approx 0.157$ and $\eta_{\mathrm{cr}} \approx 0.171$ (i.e., $\rho_{\mathrm{cr}}\sigma_1^3 = 0.132$). The low value of η_{cr} is consistent with the presence of a limited-valence mechanism[41,42]: as expected for such systems, the liquid-vapor coexistence curve appears confined to densities smaller than those generally observed in spherically attractive potentials. This circumstance suggests the presence of a region, at slightly larger densities, in which a well-defined network of bonded particles may be formed. Theoretical predictions have been obtained by repeated application of Eqs. (7) and (8) to find the coexisting densities along several isotherms; we have then estimated the critical point parameters ($T^*_{\mathrm{cr}} \approx 0.147$ and $\eta_{\mathrm{cr}} \approx 0.108$, i.e. $\rho_{\mathrm{cr}}\sigma_1^3 = 0.083$) by means of the law of rectilinear diameter and the scaling law for the densities with a non-classical critical exponent $\beta = 0.32$.[53] The RISM approach yields more

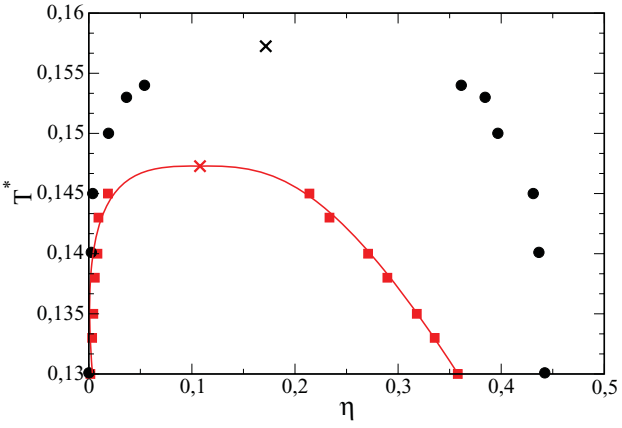

FIG. 2. GEMC (circles) and RISM (squares) liquid-vapor coexistence curves with estimates of the corresponding critical points (crosses). Full line is the interpolating curve drawn according to the scaling law for the densities and the law of rectilinear diameters. Densities in the horizontal axes are given in terms of the packing fraction $\eta = \rho V_{\mathrm{M}}$, where ρ is the number density and V_{M} is the volume of one molecule (see text). Reduced temperature on the vertical axes are defined as $T^* = k_{\mathrm{B}}T/U_0$, with U_0 the depth of the square-well attraction, see Eq. (1).

accurate predictions for the coexisting vapor densities than for the liquid ones. Similar results have already been observed for other models,[26,27,30] and reflect the tendency of the RISM/HNC to overestimate the role of repulsive forces in the overall interaction potential (and hence to overestimate the pressure) as the density increases.

We have then selected several state points in the phase diagram to investigate the local structure of the system, and the ability of the RISM theory to reproduce the simulated correlation functions. The points include a supercritical state at low density (labeled hereafter A), with $T^* = 0.30$ and $\eta = 0.130$, and several points along the high-density isochore $\eta = 0.442$, starting from the supercritical temperature $T^* = 2$, and ending in the liquid state at $T^* = 0.13$; we aim, with such analysis, to obtain a detailed picture of the short-range structuring of the fluid upon cooling. We shall first focus on two points along the isochore $\eta = 0.442$, labeled respectively B ($T^* = 0.30$, $\eta = 0.442$) and C ($T^* = 0.13$, $\eta = 0.442$).

RISM and MC data for the center-to-center radial distribution functions $g(r)$ at points A, B, and C are reported in Fig. 3. Theoretical and numerical results agree for distances larger than $r = 1.45$, the upper value separating bonded and non-bonded pairs (see below), whereas a clear discrepancy emerges for smaller distances, especially at $r = \sigma_1$, where the RISM $g(r)$ attains non-zero values in contrast with the MC evidence of vanishing correlations at those distances. Such evidence has to be ascribed to the known difficulty of the RISM to properly cope with steric effects not explicitly embodied into "atomic" site-site closures such as the envisaged HNC approximation. As a consequence, the theory allows for the (physically forbidden) possibility that two central spheres get in contact, without properly accounting for the excluded volume constraints generated by the four protruding spheres; geometrical evaluations indeed show that two central spheres cannot get closer than $r \simeq 1.09$. Comparing the $g(r)$ in A and B (see again Fig. 3), packing effects also become apparent in the progressive modulation of the radial distribution function at large r and in the structuring of the system at short range, witnessed by the presence of a small peak at $r \approx 1.2$ (absent in point A), and by the increase of $g(r)$ at $r \approx 1.42$. Upon

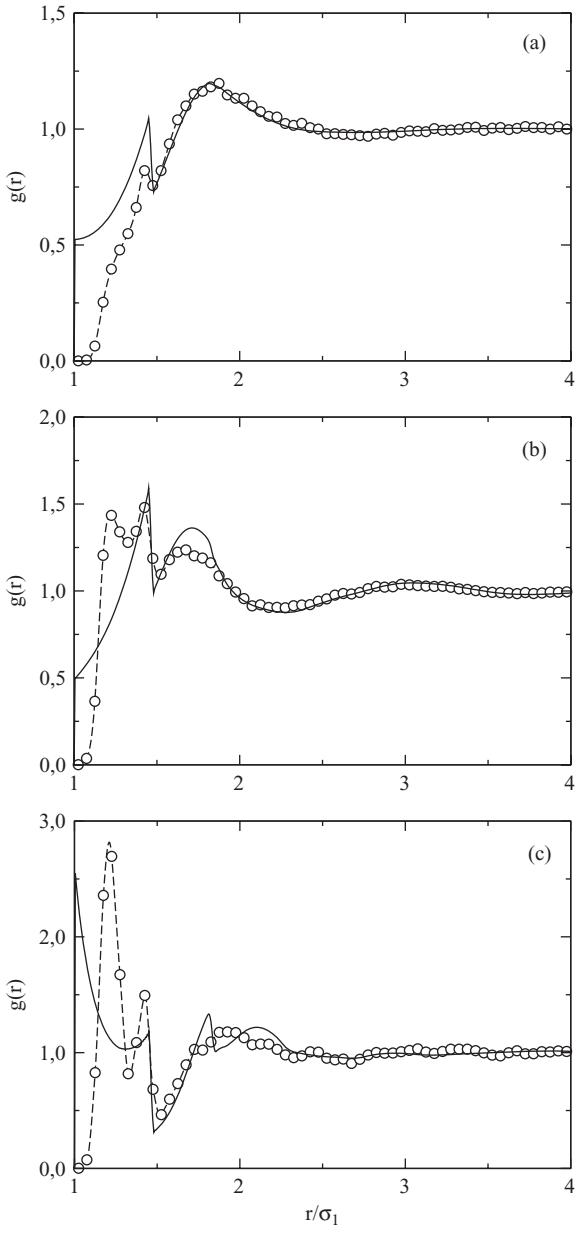

FIG. 3. MC (symbols and dashed lines) and RISM (full lines) center-to-center radial distribution function $g(r)$ at state points A (panel a, $T^* = 0.30$, $\eta = 0.130$), B (panel b, $T^* = 0.30$, $\eta = 0.442$), and C (panel c, $T^* = 0.13$, $\eta = 0.442$).

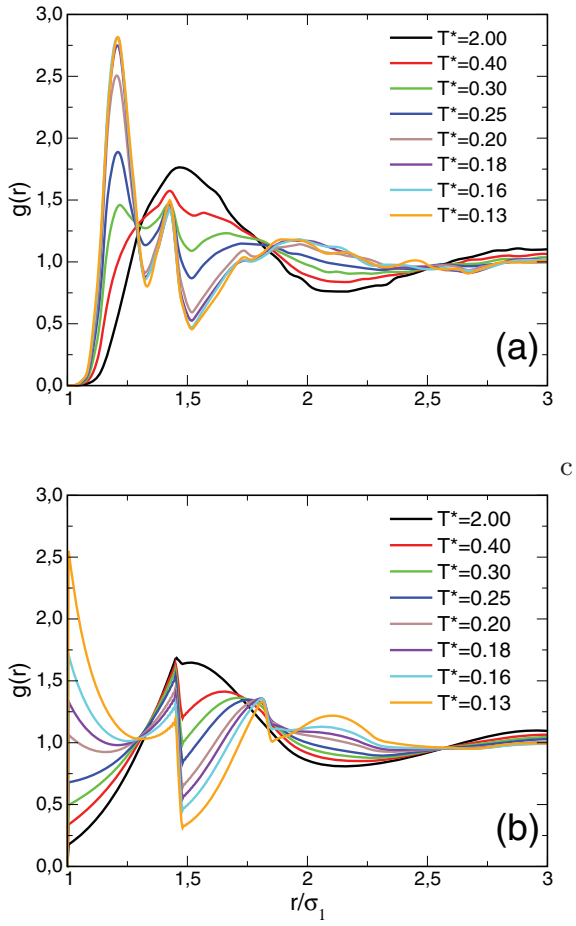

FIG. 4. MC (panel a) and RISM (panel b) $g(r)$ at $\eta = 0.442$ and different temperatures.

decreasing the temperature (point C), the fluid becomes more and more structured, as indicated by the transformation of the relatively small feature at $r = 1.2$, observed in B, into a well-defined peak in the same position. At larger distances, an additional weak peak around $r = 2.5$ is also visible in the MC data.

The emergence of a complex local order, suggested by the presence of two peaks in $g(r)$ at two close small distances, occasions a more extensive investigation of the descent in temperature along the isochoric path at $\eta = 0.442$. A comparison between MC and RISM $g(r)$ at several different temperatures, starting from $T^* = 2$, is thus reported in Fig. 4. At high temperatures, the $g(r)$ essentially reproduces a standard liquid structure, characterized by a main peak at $r \approx 1.5$ (this distance being slightly larger than $1.35\sigma_1$, i.e. the diameter of an equivalent hard sphere with volume V_M). As the temperature decreases, the progressive structuring of the fluid is signalled by the appearance of the peak at $r = 1.2$, as mentioned before, and by the splitting of the high temperature peak into two progressively sharper, different contributions, eventually placed, when $T^* \leq 0.25$, at $r = 1.42$ and 2.

PY results for $g(r)$ (not shown) turn out to be more accurate than the HNC ones in the contact region, where hard-core exclusion effects are important; however, when the attractive contributions become significant, namely upon lowering the temperature and increasing the density, the PY predictions tend to be progressively less accurate, failing to reproduce the two peaks at $r \approx 1.2$ and $r \approx 1.42$ and showing convergence problems about $T^* \simeq 0.15$.

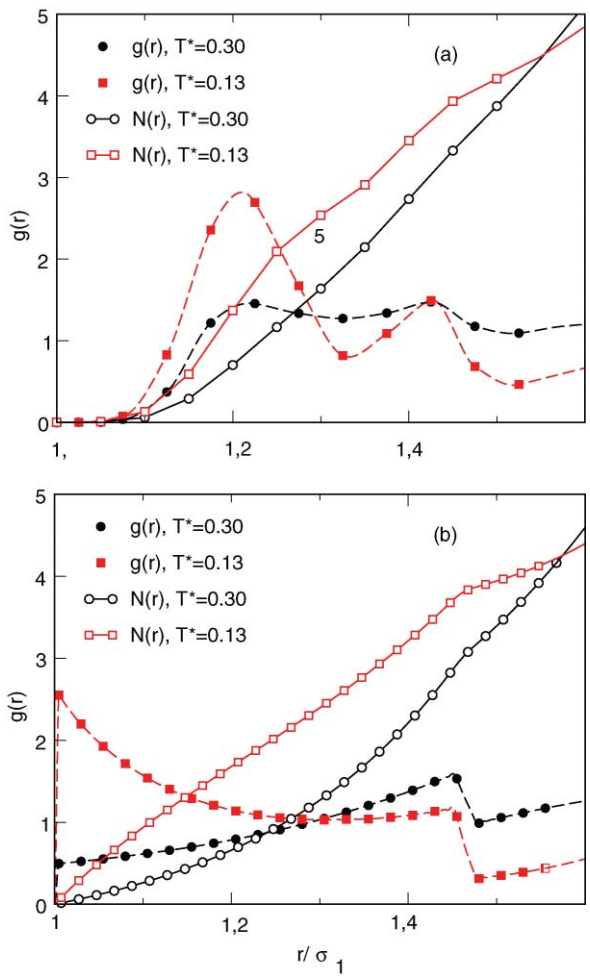

FIG. 5. MC (panel a) and RISM (panel b) coordination number $N(r)$ and $g(r)$ at state points B ($T^* = 0.30$, $\eta = 0.442$) and C ($T^* = 0.13$, $\eta = 0.442$).

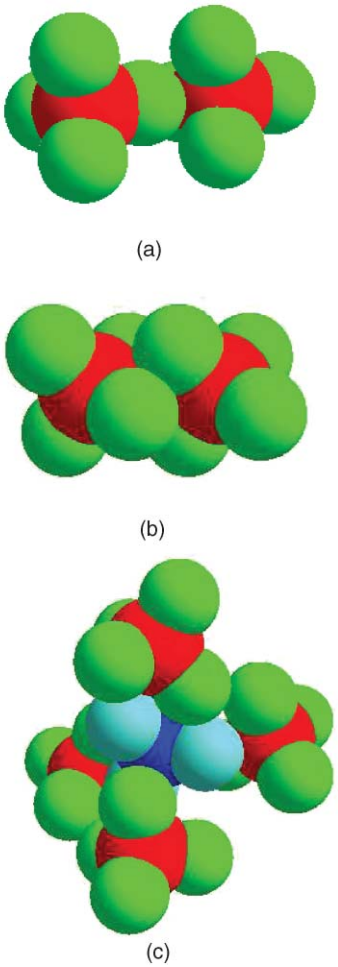

FIG. 6. Pictures of two molecules bonded in different tetrahedral arrangements, corresponding to pair interaction energies of $E_{ij} = -1$ (panel a) and $E_{ij} = -2$ (panel b). A fully bonded configuration of four particles surrounding the central particle i ($E_i = -8$), with particle i indicated by different colors, is reported in panel c.

It is instructive at this stage to examine the behavior of the coordination number $N(r)$ of central spheres: as shown in Fig. 5, for distances corresponding to the second minimum of $g(r)$, $N(r)$ goes from ~ 3 to 4, as the temperature decreases. Although $g(r)$ slightly increases after the minimum, so that a bonding region can only be roughly defined, a clear indication of a limited coordination emerges, further supporting our hypothesis that the model belongs to the class of low-valence systems. Actually, further RISM calculations (not reported here) demonstrate that $N(r)$ has a well-defined plateau ~ 4 for $T^* \approx 0.05$, a temperature prohibitively low to be investigated via standard simulation techniques.

The sequence of the peaks visible in Fig. 4 and the evolution of $N(r)$ from point B to C in Fig. 5 appear compatible with the superposition of two different short-range orders. The first one, depicted in panel (a) of Fig. 6, consists in a collinear arrangement of two central spheres, separated by an

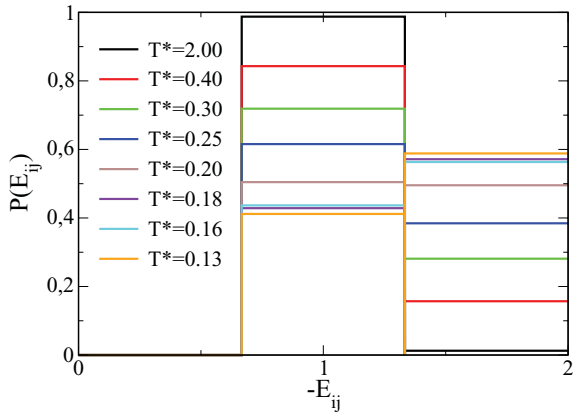

FIG. 7. Distribution of single ($E_{ij} = -1$) and double ($E_{ij} = -2$) bonds at fixed $\eta = 0.442$ and different temperatures.

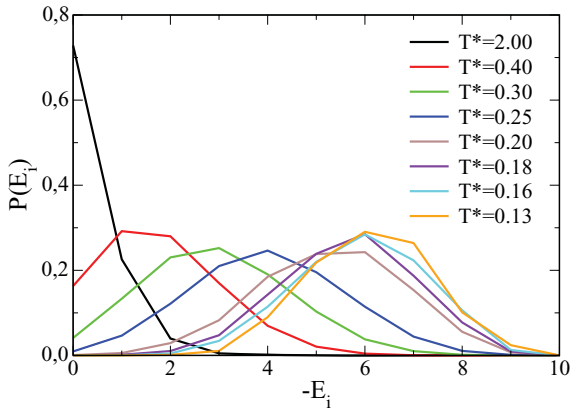

FIG. 8. Histogram of the total energy per particle E_i at fixed $\eta = 0.442$ and different temperatures.

external one placed between them, consistently with the presence of a peak in $g(r)$ at $r = 1.42$. In this case, the pair interaction energy is $E_{ij} = -U_0$. A second tighter arrangement, shown in panel (b) of Fig. 6, is obtained when two central spheres approach to each other down to $r = 1.2$ (the position of the main peak), i.e., almost to the minimum allowed distance 1.09, discussed above. In this configuration the interacting pair forms two bonds, involving simultaneously the two central spheres and two external spheres and thus the pair interaction energy is $E_{ij} = -2U_0$. Interestingly enough, the third and fourth peak in $g(r)$ are at about 1.63 times the values $r = 1.2$ and 1.42, respectively, suggesting that both configurations favor a local tetrahedral arrangement.

The distribution of single ($E_{ij} = -U_0$) and double bonds ($E_{ij} = -2U_0$) at $\eta = 0.442$, reported in Fig. 7, suggests that progressively more and more single bonds turn into double bonds as the temperature decreases.

Additional information on the bonding geometries can be obtained from the distribution of the energy per particle, calculated as the sum of the pair interaction energies of all j neighbors of a given i molecule, i.e., $E_i \equiv \sum_j E_{ij}$. Results are shown in Fig. 8: at high temperatures, the distribution has a maximum at $E(i) = 0$, testifying the practical absence of bonding in the system. The maximum shifts towards higher energies as the temperature decreases, and attains the value ≈ 0.3 at $E_i \approx 6$ for $T^* = 0.13$, signaling the onset of a geometrical arrangement where one molecule is coordinated with four neighbors, two of which linked with a single bond and the other two with a double bond (giving, as already stated, a total energy value of $-6U_0$). The progressive shift of the maximum position towards greater energies suggests that a fully tetrahedral network (in which a molecule is involved in four double bonds, with a resulting energy of $-8U_0$) might be realized at even lower temperatures; this expectation is consistent with the RISM indication we have alluded to, of a sharply defined tetrahedral coordination at $T^* = 0.05$. A graphical representation of five molecules involved in a fully bonded configuration is shown in panel (c) of Fig. 6.

Next, we compare in Fig. 9 RISM and MC results for the center-to-center static structure factor $S(k)$. The panel (a) shows the MC data. At high temperatures, the MC $S(k)$ displays a main peak at $k \approx 4.5$ that tends to decrease upon cooling, eventually evolving into two separate peaks, namely a small feature at $k = 4.5$ and a well-defined peak at $k = 6.5$. The RISM/HNC $S(k)$ (panel b) qualitatively reproduces the MC trends, including the presence and the evolution of the two peaks at $k = 3.7$ and 6.5; the former appears more pronounced and shifted towards lower k, in comparison with MC data. In the low-k region, $S(k)$ is relatively small, consistently with the fact that the investigation is carried relatively far from the binodal region. Conversely, we have verified that the PY closure is not able to reproduce the splitting of the main peak of $S(k)$.

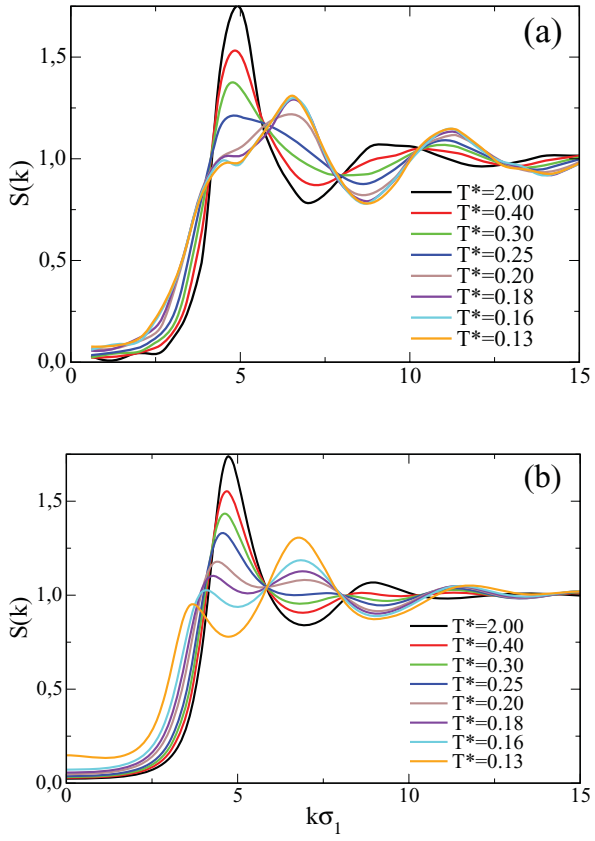

FIG. 9. MC (panel a) and RISM (panel b) center-to-center static structure factor $S(k)$ at fixed $\eta = 0.442$ and different temperatures.

IV. CONCLUSIONS

We have investigated a system of tetrahedrally shaped molecules, constituted by five partially fused hard spheres, by means of Monte Carlo simulations and the RISM theory of molecular fluids. The intermolecular arrangement arises from the competition between hard-core excluded volume effects and a (short-range) square-well attraction acting between the central sphere of one molecule and the four outer spheres of another molecule.

Simulation and theory signal the onset, at sufficiently low temperatures, of two different tetrahedral arrangements, namely, (i) a fully bonded configuration, where the central sphere of a given molecule is in contact with two outer spheres of each of the neighbour molecules and (ii) a more open structure, where a central sphere of a given molecule is in contact with only one outer sphere of each of the neighbours. The two arrangements coexist in the temperature range we have investigated, with the open structure progressively giving place to the fully bonded one as the temperature decreases.

The self-assembly of colloidal systems in tetrahedral structures is of interest for the synthesis of colloidal crystals with a diamond structure, a property of crucial importance for innovative photonic applications.[55,56] For this reason it would be interesting to ascertain whether the present model is able to form a tetrahedral crystalline structure upon approaching freezing, and, if so, whether the twofold packing evidenced in the liquid could be traced also in the solid phase. We are currently planning appropriate strategies to investigate this point.

As for the accuracy of the RISM, theoretical predictions appear qualitatively satisfactory. Indeed, the theory reproduces the split of the main peak of the structure factor at low temperatures, a feature intimately related to the onset of the tetrahedral order. This result does not appear as an obvious outcome and in fact, previous theoretical attempts were unsuccessful in this respect: one based on a Percus-Yevick description of a two-component fluid system, mimicking the envisaged colloidal model,[23] and another one—yet unpublished—where we have employed the more sophisticated modified-hypernetted chain scheme. It is worth noting that the RISM evidence for the split of the structure factor turns out to be restricted to a relatively narrow range of the thermodynamic parameter space; hence, the onset of the tetrahedral order depends on rather peculiar combinations of temperature and density.

On the other hand, the RISM predictions for the liquid-vapor coexistence and for the short-range correlations are less satisfactory. As for the binodal, liquid-branch densities appear generally underestimated, testifying the tendency of the theory to overtake the repulsive interactions; as for the radial distribution functions, the theory allows for a forbidden contact between the inner spheres of two different molecules, a well-known inconsistency related to the "atomistic" nature of closures such as the HNC employed in this work. Such intrinsic limitations could be possibly overcome through more sophisticated variants of the basic RISM formalism, such as the "diagrammatic proper" formulation of the theory[57] or the use of so-called "molecular closures," already successfully implemented for the contracted formalism known as pRISM[58] We are currently investigating the possibility to extend such schemes to the present context.

[1] D. J. Kraft, W. S. Vlug, C. M. van Kats, A. van Blaaderen, A. Imhof, and W. K. Kegel, J. Am. Chem. Soc. **131**, 1182 (2009).
[2] Y.-S. Cho, G.-R. Yi, J.-M. Lim, S.-H. Kim, V. N. Manoharan, D. J. Pine, and S.-M. Yang, J. Am. Chem. Soc. **127**, 15968 (2005).
[3] L. Hong, A. Cacciuto, E. Luijten, and S. Granick, Langmuir **24**, 621 (2008).
[4] Q. Chen, S. C. Bae, and S. Granick, Nature (London) **469**, 381 (2011).
[5] J. Lyklema, *Fundamentals of Interface and Colloidal Science* (Academic, London, UK, 1991).
[6] A. Giacometti, F. Lado, J. Largo, G. Pastore, and F. Sciortino, J. Chem. Phys. **132**, 174110 (2010).
[7] F. Sciortino, A. Giacometti, and G. Pastore, Phys. Rev. Lett. **103**, 237801 (2009).
[8] Z. Zhang and S. C. Glotzer, Nano Lett. **4**, 1407 (2004).
[9] A. B. Pawar and I. Kretzschmar, Langmuir **24**, 355 (2008).
[10] E. Bianchi, R. Blaak, and C. Likos, Phys. Chem. Chem. Phys. **13**, 6397 (2011).
[11] N. Kern and D. Frenkel, J. Chem. Phys. **118**, 9882 (2003).
[12] C. De Michele, S. Gabrielli, P. Tartaglia, and F. Sciortino, J. Phys. Chem. B **110**, 8064 (2006).
[13] J. P. K. Doye, A. A. Louis, I.-C. Lin, L. R. Allen, E. G. Noya, A. W. Wilber, H. C. Kok, and R. Lyus, Phys. Chem. Chem. Phys. **9**, 2197 (2007).
[14] A. Giacometti, F. Lado, J. Largo, G. Pastore, and F. Sciortino, J. Chem. Phys. **131**, 174114 (2009).
[15] W. R. Smith and I. Nezbeda, J. Chem. Phys. **81**, 3694 (1984).
[16] J. Kolafa and I. Nezbeda, Mol. Phys. **61**, 161 (1987).
[17] F. Sciortino, Collect. Czech. Chem. Commun. **75**, 349 (2010).
[18] J. P. Hansen and I. R. McDonald, *Theory of Simple Liquids*, 3rd Ed. (Academic, New York, 2006).
[19] C. Caccamo, Phys. Rep. **274**, 1 (1996).
[20] F. Lado, Phys. Rev. A **8**, 2548 (1973).
[21] Y. V. Kalyuzhnyi, H. Docherty, and P. T. Cummings, J. Chem. Phys. **133**, 044502 (2010).
[22] C. Gögelein, G. Nägele, R. Tuinier, T. Gibaud, A. Stradner, and P. Schurtenberger, J. Chem. Phys. **129**, 085102 (2008).
[23] E. Zaccarelli, F. Sciortino, and P. Tartaglia, J. Chem. Phys. **127**, 174501 (2007).
[24] D. Chandler and H. C. Andersen, J. Chem. Phys. **57**, 1930 (1972).
[25] L. J. Lowden and D. Chandler, J. Chem. Phys. **61**, 5228 (1974).
[26] L. Lue and D. Blankschtein, J. Chem. Phys. **102**, 5427 (1995).
[27] A. Kovalenko and F. Hirata, J. Theor. Comput. Chem. **1**, 381 (2002).
[28] B. M. Pettitt and P. J. Rossky, J. Chem. Phys. **78**, 7296 (1983).
[29] B. Kvamme, Phys. Chem. Chem. Phys. **4**, 942 (2002).
[30] D. Costa, G. Munaò, F. Saija, and C. Caccamo, J. Chem. Phys. **127**, 224501 (2007).
[31] G. Munaò, D. Costa, F. Saija, and C. Caccamo, J. Chem. Phys. **132**, 084506 (2010).
[32] L. Harnau, J.-P. Hansen, and D. Costa, Europhys. Lett. **53**, 729 (2001).
[33] D. Costa, J.-P. Hansen, and L. Harnau, Mol. Phys. **103**, 1917 (2005).
[34] J. P. Hansen and C. Pearson, Mol. Phys. **104**, 3389 (2006).
[35] L. V. Z. P. G. Khalatur and A. R. Khokhlov, J. Phys. II **7**, 543 (1997).
[36] W. Kung, P. González-Mozuelos, and M. O. de la Cruz, Soft Matter **6**, 331 (2010).
[37] P. A. Monson and G. P. Morriss, Adv. Chem. Phys. **77**, 451 (1990).
[38] F. Hirata, *Molecular Theory of Solvation* (Kluwer Academic, Dordrecht, The Netherlands, 2003).
[39] T. Miyata, Y. Ikuta, and F. Hirata, J. Chem. Phys. **133** (2010).
[40] S. Ten-no, J. Jung, H. Chuman, and Y. Kawashima, Mol. Phys. **108**, 327 (2010).
[41] E. Zaccarelli, S. V. Buldyrev, E. La Nave, A. J. Moreno, Saika-Voivod, F. Sciortino, and P. Tartaglia, Phys. Rev. Lett. **94**, 218301 (2005).
[42] E. Bianchi, J. Largo, P. Tartaglia, E. Zaccarelli, and F. Sciortino, Phys. Rev. Lett. **97**, 168301 (2006).
[43] B. Ruzicka, E. Zaccarelli, L. Zulian, R. Angelini, M. Sztucki, A. Moussaïd, T. Narayanan, and F. Sciortino, Nature Mater. **10**, 56 (2011).
[44] E. Bianchi, G. Kahl, and C. N. Likos, (unpublished).
[45] F. Hirata, B. M. Pettitt, and P. J. Rossky, J. Chem. Phys. **77**, 509 (1982).

[46]W. R. Smith, D. Henderson, and R. D. Murphy, J. Chem. Phys. **61**, 2911 (1974).
[47]W. R. Smith and D. Henderson, J. Chem. Phys. **69**, 319 (1978).
[48]F. O. Raineri and G. Stell, J. Phys. Chem. B **105**, 11880 (2001).
[49]S. J. Singer and D. Chandler, Mol. Phys. **55**, 621 (1985).
[50]T. Morita and K. Hiroike, Prog. Theor. Phys. **23**, 1003 (1960).
[51]A. Kovalenko and F. Hirata, Chem. Phys. Lett. **349**, 496 (2001).
[52]A. Z. Panagiotopoulos, Mol. Phys. **61**, 813 (1987).
[53]B. Smith and D. Frenkel, *Understanding Molecular Simulations* (Academic, New York, 1996).
[54]N. B. Wilding, J. Phys.: Condens. Matter **9**, 585 (1996).
[55]M. Maldovan and E. L. Thomas, Nature Mater. **3**, 593 (2004).
[56]K. M. Ho, C. T. Chan, and C. M. Soukoulis, Phys. Rev. Lett. **65**, 3152 (1990).
[57]D. Chandler, R. Silbey, and B. Ladanyi, Mol. Phys. **46**, 1335 (1982).
[58]K. S. Schweizer and A. Yethiraj, J. Chem. Phys. **98**, 9053 (1993).